Application of pole decomposition to an equation governing the dynamics of wrinkled flame fronts

Olivier Thual, U. Frisch, M. Hénon

J. Physique **46** (1985) 1485-1494 SEPTEMBRE **1985**, PAGE 1485

Classification
Physics Abstracts
05.45 — 47.20 — 47.70F

Application of pole decomposition to an equation governing the dynamics of wrinkled flame fronts

O. Thual

CNRM, 42 avenue Coriolis, 31057 Toulouse Cedex, France

U. Frisch and M. Hénon

CNRS, Observatoire de Nice, B.P. 139, 06003 Nice Cedex, France

(*Reçu le 27 février 1985, accepté le 13 mai 1985*)

Résumé. — L'équation intégrale de Sivashinsky gouvernant certaines instabilités hydrodynamiques de fronts de flamme unidimensionnels est un cas particulier des modèles de plasma non linéaires de Lee et Chen ; en tant que telle elle possède une décomposition en pôles. Ceci explique les structures très organisées observées dans les simulations numériques. L'équation de Sivashinsky a des solutions stationnaires stables avec les pôles alignés parallèlement à l'axe imaginaire. Avec des conditions aux limites périodiques, quand le nombre de modes linéairement instables est élevé, les pôles se condensent en une distribution ln coth. Ceci est illustré par calcul numérique des positions d'équilibre des pôles. La condensation des pôles explique les plis de certains fronts de flamme. Le spectre d'énergie du déplacement du front suit une loi en $\ln^2 k$.

Abstract. — The Sivashinsky integral equation governing certain hydrodynamical instabilities of one-dimensional flame fronts is a special case of Lee and Chen's (*Phys. Scr.* **2** (1982) 41) non linear plasma models ; as such it has a pole decomposition. This explains the highly organized structures observed in numerical simulations. The Sivashinsky equation has stable steady solutions with the poles aligned parallel to the imaginary axis. With periodic boundary conditions, when the number of linearly unstable modes is large, the poles condense into a ln coth distribution. This is illustrated by numerical calculations of equilibrium positions of poles. The pole condensation explains cusp-like wrinkles in certain flame fronts. The energy spectrum for the front displacement follows a $\ln^2 k$ law.

1. Introduction.

Sivashinsky [1] has shown that in a suitable asymptotic regime the dynamics of wrinkled flame fronts is governed by a non linear partial (pseudo)differential equation. In the one-dimensional case it reads

$$\partial_t u + u\,\partial_x u = \Lambda u + \nu\,\partial_x^2 u\,. \qquad (1.1)$$

Λ is a linear singular operator defined conveniently in terms of the spatial Fourier transform :

$$u(t, x) = \int_{-\infty}^{+\infty} e^{ikx}\,\hat{u}(t, k)\,dk\,, \qquad (1.2)$$

by

$$\Lambda : \hat{u}(t, k) \mapsto |k|\,\hat{u}(t, k)\,. \qquad (1.3)$$

We here use notation different from Sivashinsky's in order to bring out similarities with Burgers' equation

$$\partial_t u + u\,\partial_x u = \nu\,\partial_x^2 u\,. \qquad (1.4)$$

What is here denoted u is actually not a velocity but $\partial_x \phi$ where ϕ is the flame front displacement ; so it is the slope of the flame front. Also we find it more convenient to vary the « viscosity » ν rather than the size of the domain.

Various studies of the Sivashinsky equation have been reported [1-4]. The results indicate that the solutions are highly organized in the form of one or several wrinkles (see Figs. 2 and 3 of Ref. [3] and also Figs. 2 and 3 of the present paper).

At the root of this simple behaviour of the Sivashinsky equation is the fact that it possesses a *pole decomposition* : equation (1.1) admits solutions of the

form

$$u(t, x) = -2\nu \sum_{\alpha=1}^{2N} \frac{1}{x - z_\alpha(t)}. \quad (1.5)$$

The z_α's are poles in the complex plane (coming in c.c. pairs) moving according to the laws of motion of poles ($\alpha = 1, 2, ..., 2N$)

$$\dot{z}_\alpha = -2\nu \sum_{\beta \neq \alpha} \frac{1}{z_\alpha - z_\beta} - i \,\mathrm{sign}\,(\Im(z_\alpha)), \quad (1.6)$$

where $\Im$ denotes the imaginary part. When 2π spatial periodicity is assumed it is enough to restrict attention to poles with real parts between 0 and 2π. Instead of equations (1.5) and (1.6) one then uses

$$u(t, x) = -\nu \sum_{\alpha=1}^{2\pi} \cot\left(\frac{x - z_\alpha}{2}\right) \quad (1.7)$$

and

$$\dot{z}_\alpha = -\nu \sum_{\beta \neq \alpha} \cot\left(\frac{z_\alpha - z_\beta}{2}\right) - i \,\mathrm{sign}\,(\Im(z_\alpha)). \quad (1.8)$$

The existence of this pole decomposition follows from a more general result of Lee and Chen [5] for a class of non linear dynamical models arising in plasma turbulence. In our notation the governing equations for the Lee and Chen models are

$$\partial_t u + u\,\partial_x u = \nu\,\partial_x^2 u + \rho \Lambda u + \sigma \Lambda\,\partial_x u, \quad (1.9)$$

which is a linear combination of the Sivashinsky equation and the Benjamin-Ono [6-7] equation. For the convenience of the reader a derivation of the pole decomposition for the Sivashinsky equation is given in the appendix A.

We shall not here review work on pole decompositions. A list of references up to 1981 may be found in section 4 of reference [8]. We also mention a recent application of pole decomposition to the formation of cusp singularities in interface dynamics [9].

This paper is organized as follows : section 2 is a systematic study of the two pole problem giving some qualitative insight into N-pole dynamics; in particular there is a tendency for the poles to align themselves parallel to the imaginary axis. Subsequently the paper is devoted essentially to the detailed study of such « vertical alignments ». Section 3 is about the discrete dynamics of N pairs of poles : for N large the poles condense into a continuous distribution which is determined analytically (Sect. 4). This is the analog for the Sivashinsky equation of the pole condensations for Burgers' equation [10]. From the distribution of poles we deduce the shape of flame wrinkles and the high wavenumber behaviour of the energy spectrum. In section 5 we mention some implications and open problems.

2. The two-pole problem and qualitative dynamics.

We begin by studying the simplest dynamical situation with two poles at complex conjugate locations $z(t) = a(t) + ib(t)$ and $z_* = a - ib$ with $b > 0$. From equation (1.6), we have

$$\dot{z} = -\frac{2\nu}{z - z_*} - i. \quad (2.1)$$

It follows that a is a constant and that

$$\dot{b} = \frac{\nu}{b} - 1. \quad (2.2)$$

Note that the $-2\nu/(z - z_*)$ term in equation (2.1), already present in Burgers' dynamics, tends to push the poles away from the real axis while the $-i$ term produces a uniform drift towards the real axis. Their competition leads for $t \to \infty$ to a stable equilibrium configuration with

$$b_{eq} = \nu. \quad (2.3)$$

The corresponding steady solution of the Sivashinsky equation is

$$u(x) = -\frac{4\nu x}{x^2 + \nu^2}. \quad (2.4)$$

In the periodic case equations (2.3) and (2.4) become respectively

$$b_{eq} = \operatorname{arg\,tanh} \nu, \quad (2.5)$$

and

$$u(x) = -\frac{2\nu \sin x}{(1 - \nu^2)^{-1/2} - \cos x}. \quad (2.6)$$

A graph of $u(x)$ for $\nu = 5 \times 10^{-2}$ is shown in figure 1. The aspect is quite similar to the localized structures appearing in figure 3 of reference [4], concerning an equation differing very slightly from the Sivashinsky equation.

Next we consider two poles z_1 and z_2 in the upper half plane $\Im(z) > 0$ which we assume to be sufficiently close to each other so that we can ignore their interactions with other poles. We then have

$$\dot{z}_1 = -\frac{2\nu}{z_1 - z_2} - i, \quad \dot{z}_2 = -\frac{2\nu}{z_2 - z_1} - i. \quad (2.7)$$

Thus $\zeta = z_1 - z_2 = a + ib$ satisfies

$$\dot{\zeta} = -\frac{4\nu}{\zeta}. \quad (2.8)$$

Hence

$$\zeta^2(t) - \zeta^2(0) = -8\nu t. \quad (2.9)$$

When t varies from 0 to $+\infty$, then $\Im(\zeta^2) = 2ab$ remains constant so that the point (a, b) moves on a

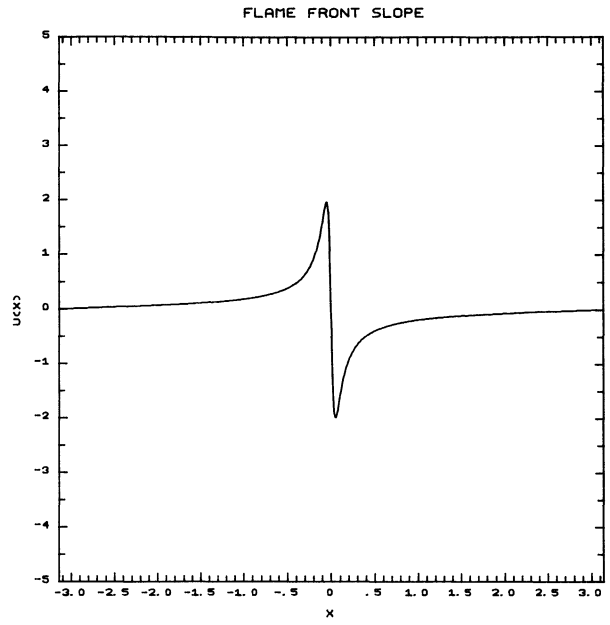

Fig. 1. — Structure of the slope of the flame front $u(x)$ for the steady space-periodic solution with two complex conjugate poles.

hyperbola. For large times $a \to 0$ and $b \to +\infty$: poles tend to align on a parallel to the imaginary axis.

The above analysis indicates that, roughly, poles tend to attract each other horizontally (parallel to the real axis) and to repel each other vertically. In addition, they are subject to a drift towards the real axis. Extrapolation of these qualitative features to a situation with many poles suggests that the poles tend to form vertical alignments, eventually coalescing into a single one. This is indeed happening in Burgers' dynamics and may be viewed as the mechanism for the formation and coalescence of shocks. According to Lee and Chen [5] this merging process is a universal property of their non dispersive models.

In the periodic case the poles are constrained to be on 2π periodic arrays or, equivalently, to be all contained in a domain of extension 2π in the real direction and to have cot rather than z^{-1} interactions. The short distance behaviour is thus unaffected, but the global dynamics are quite different. At the moment there is no result concerning the eventual fate of a system of poles (periodic or non periodic). In the periodic case numerical integrations of the Sivashinsky equation [3-4] indicate that for small ν the solutions often tend to a steady state with one or several wrinkles in the flame front displacement (in fact vertical pole condensations as we shall see). These features are reproduced in simulations of our own using a pseudo-spectral method with 512 Fourier modes. Figure 2 shows a solution with one wrinkle for $\nu = 0.1$. Figure 3 shows a solution with two wrinkles, also for $\nu = 0.1$, but restricted to the class of functions $u(x)$ which are odd (otherwise this solution would be unstable). The labels a and b correspond respectively to the front displacement $\phi(x)$ and the front slope $u(x)$.

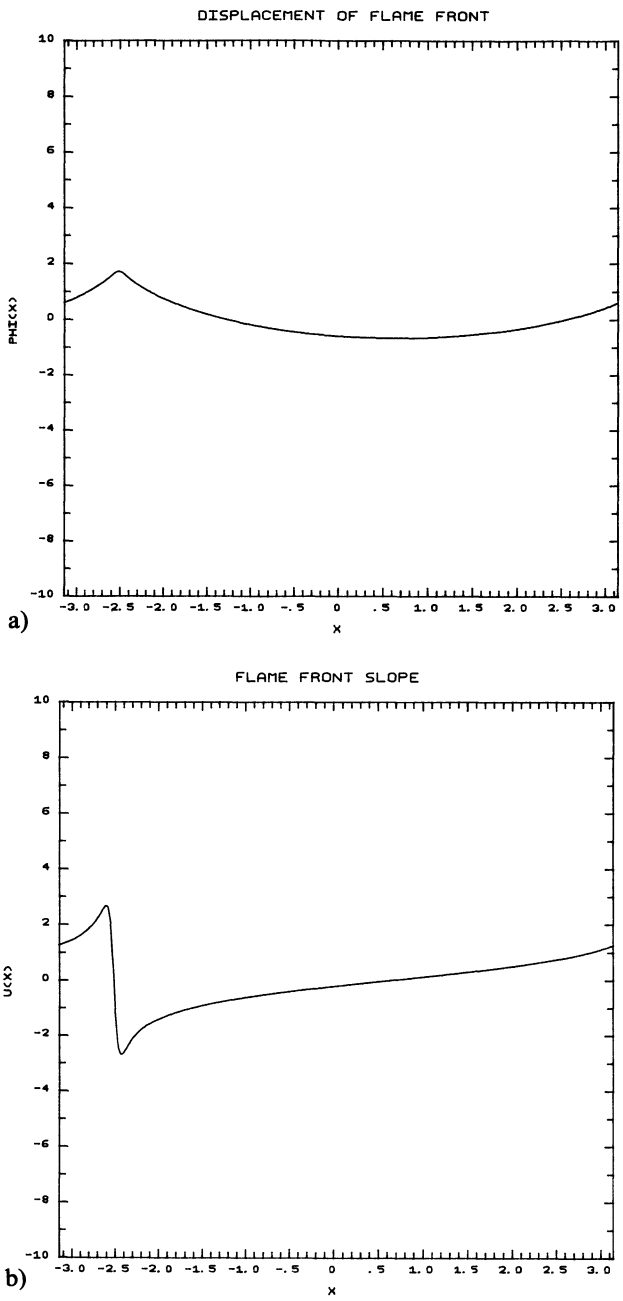

Fig. 2. — Structure of the flame front (a) and its slope (b) for a steady one-wrinkle space-periodic solution obtained by pseudo-spectral simulation of the Sivashinsky equation with 512 Fourier modes and « viscosity » coefficient $\nu = 0.1$.

Henceforth we shall consider a single vertical alignment, possibly containing a large number of poles, with or without periodicity.

3. Vertical alignments of poles : discrete dynamics.

We consider N pairs of complex conjugate poles constrained to be on a parallel to the imaginary axis, located at

$$x = x_0\,, \quad y = \pm\, y_1, \ldots, \pm\, y_N\,. \qquad (3.1)$$

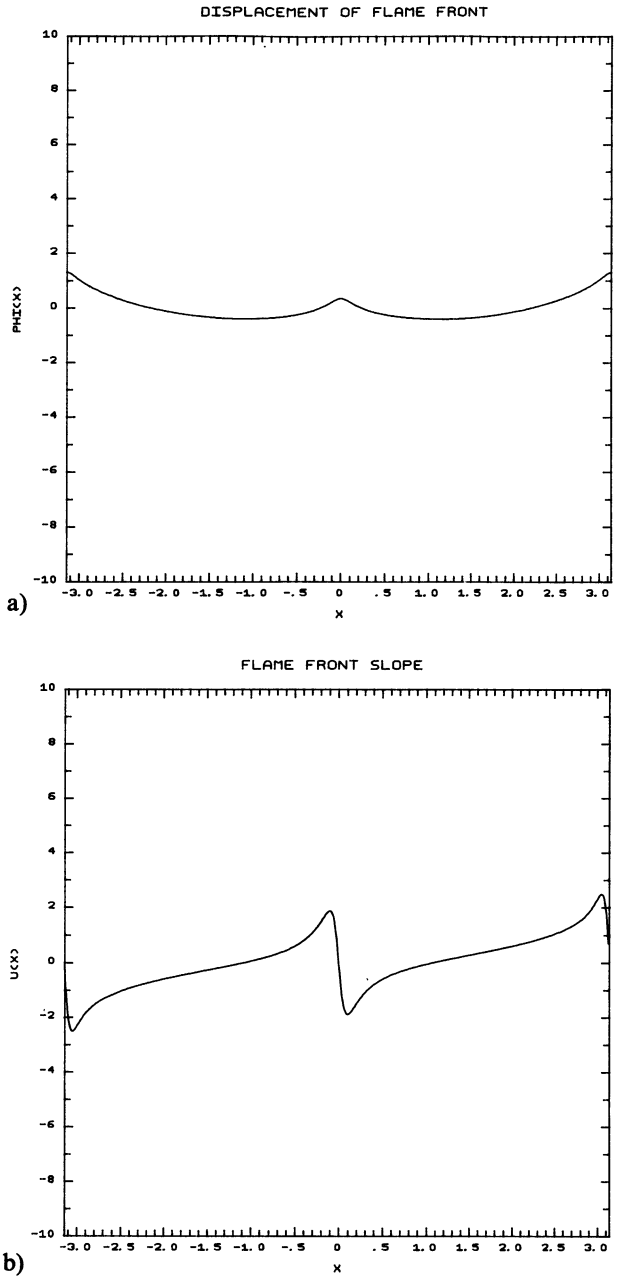

Fig. 3. — Same as figure 2, except that the solution $u(x)$ is restricted to odd functions, allowing stable coexistence of two wrinkles.

Without loss of generality, we assume that $x_0 = 0$; we also assume that the y_j's have been ordered :

$$0 < y_1 < \cdots < y_N . \tag{3.2}$$

This order will never change since the repulsion between two poles becomes infinite when they approach each other. For the same reason, we always have strict inequalities in (3.2).

The motion of poles is given by a set of N simultaneous real differential equations :

$$\dot{y}_j = f_j(y_1, \ldots, y_N) , \tag{3.3}$$

with, in the non-periodic case

$$f_j = v\left[\frac{1}{y_j} + \sum_{k \neq j}\left(\frac{2}{y_j - y_k} + \frac{2}{y_j + y_k}\right)\right] - 1 , \tag{3.4}$$

and in the periodic case

$$f_j = v\left[\coth y_j + \sum_{k \neq j}\left(\coth\frac{y_j - y_k}{2} + \coth\frac{y_j + y_k}{2}\right)\right] - 1 . \tag{3.5}$$

For $N = 1$, (3.4) reduces to (2.2). A steady state will be a solution of the N simultaneous ordinary equations

$$f_j = 0 \quad (i = 1, \ldots, N) . \tag{3.6}$$

We note first some properties of these equations.

(i) In the non-periodic case, v can be eliminated by the change of variables

$$y_j = vY_j , \quad t = vT . \tag{3.7}$$

v is therefore an irrelevant parameter. On the contrary, in the periodic case a scale is prescribed so that the value of v is relevant.

(ii) In the non-periodic case, multiplying (3.4) by y_j and summing over j, we obtain the virial-like relation

$$\frac{1}{2}\frac{\mathrm{d}}{\mathrm{d}t}\sum_{j=1}^{N} y_j^2 = vN(2N - 1) - \sum_{j=1}^{N} y_j . \tag{3.8}$$

The right-hand side must vanish at equilibrium; this provides a test of computational accuracy.

(iii) In the periodic case, we derive from (3.5) for the highest pole $j = N$, using the fact that

$$\coth x > 1 \quad \text{for} \quad x > 0 :$$

$$f_N > v(2N - 1) - 1 . \tag{3.9}$$

If the right-hand side is positive or zero, f_N is always positive, and no steady state can exist; the highest pole moves towards $y = +\infty$ in the imaginary direction with an (asymptotically) constant speed. Therefore a necessary condition for the existence of a steady state in the periodic case is

$$v(2N - 1) < 1 . \tag{3.10}$$

(iv) The following properties hold in the non-periodic case, and also in the periodic case when (3.10) is satisfied :

1. *There exists one and only one steady state.*

2. *Any solution of* (3.3) *tends towards the steady state for* $t \to +\infty$. The proof of these properties is based on the existence of a Lyapunov function (see Appendix B).

(v) The equations (3.6) are easily solved for $N = 1, 2, 3$ in the non-periodic case. We take $v = 1$ for simplicity. For $N = 1$, the steady state solution is

$$y_1 = 1 . \tag{3.11}$$

For $N = 2$:

$$y_1 = 3 - \frac{3\sqrt{2}}{2} = 0.878680...,$$

$$y_2 = 3 + \frac{3\sqrt{2}}{2} = 5.121320.... \quad (3.12)$$

For $N = 3$, the y_j are the three roots of the equation

$$y^3 - 15\,y^2 + \frac{45 + 15\sqrt{129}}{4}\,y - \frac{135\sqrt{129} - 1\,395}{4} = 0, \quad (3.13)$$

i.e.

$$y_1 = 0.818742..., \quad y_2 = 4.254082..., \quad y_3 = 9.927176... \quad (3.14)$$

These valus can also be used as a check on the program for the numerical solution of (3.6).

We turn now to numerical determination of the equilibrium positions. The equations (3.6) were solved numerically by a relaxation method : the position y_i of each pole in turn is adjusted to a new value

$$y'_j = y_j + \Delta y_j . \quad (3.15)$$

Δy_j is computed by a one-step Newton formula :

$$\Delta y_j = - f_j \left(\frac{\partial f_j}{\partial y_j}\right)^{-1}, \quad (3.16)$$

with the constraint that it should not exceed one-half of the distance to the next pole. A convenient initial state is : $y_j = 2\,vj$. The computation is halted when the relative change $|\Delta y_j|/y_j$ becomes less than some prescribed small number for all poles. This method was found to always converge to the equilibrium, although the convergence slows down for large N.

The value

$$v = 0.005 \quad (3.17)$$

was used in all numerical computations, in order to facilitate comparisons. As a consequence of (3.10), a small value of v is necessary in order to allow a large number of poles in the periodic case. With the value (3.17), the maximum of N in the periodic case is

$$N_{max} = 100 . \quad (3.18)$$

Figures 4a and 4b show (full curves) the cumulative distribution, i.e., the number of poles between 0 and y as a function of y, for the non-periodic case and for $N = 10$ and $N = 100$ respectively. The dotted and dashed curves are analytic approximations which will be described in section 4. Table I gives in columns 2 and 3 the positions of the lowest and highest poles, y_1 and y_N, for various N. Column 4 is an analytic estimate which will also be described in section 4.

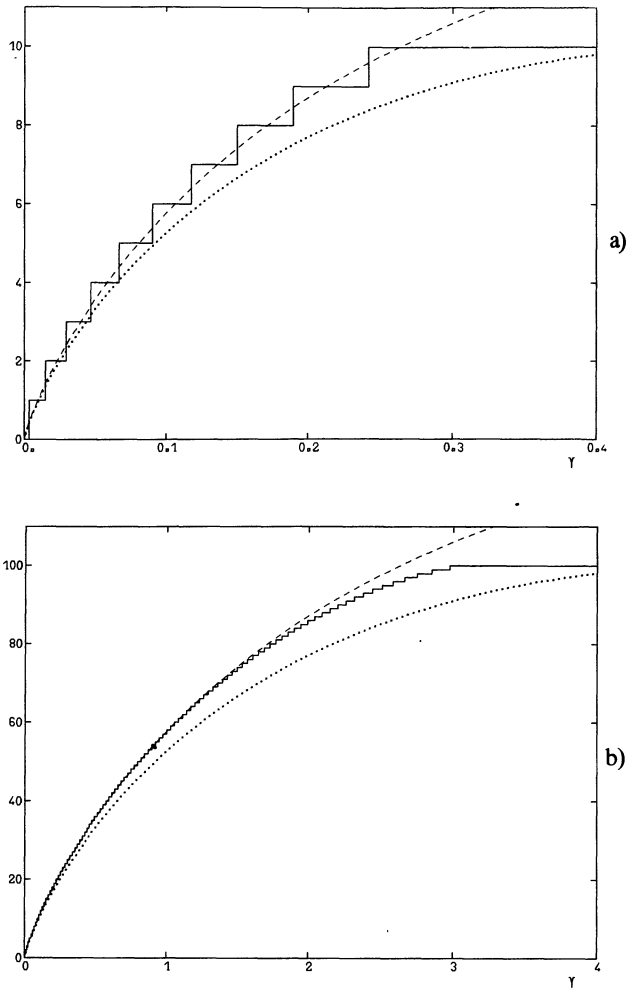

Fig. 4. — Cumulative distribution of poles along the imaginary axis in the non-periodic case. Full curve (staircase) : discrete distribution for (a) $N = 10$, (b) $N = 100$. Dotted and dashed curves : asymptotic distribution (4.5) with normalization given respectively by (4.4) and (4.6).

Table I

N	y_1	y_N	y_1^*
1	0.005000	0.005000	0.008070
2	0.004393	0.025607	0.006129
3	0.004094	0.049636	0.005417
4	0.003902	0.075278	0.005016
5	0.003764	0.10188	0.004747
10	0.003387	0.24178	0.004084
20	0.003076	0.53470	0.003596
50	0.002740	1.4409	0.003115
100	0.002531	2.9761	0.002833
200	0.002351	6.0730	0.002600

In the periodic case, when N is well below N_{max}, the distribution differs only slightly from the non-periodic case. For $N = 10$, for instance, one obtains a curve which is barely distinguishable from that of figure 4*a*. The reason is simply that for small y, (3.5) reduces to (3.4). As N increases and approaches N_{max}, however, the periodic case deviates from the non-periodic case. Figure 5 shows the cumulative distribution of the periodic case for $N = N_{max} = 100$. This distribution differs noticeably from that of figure 4*b* (the horizontal scale is not the same). The dashed curve is again an analytic approximation which will be described in section 4. Table II gives the positions of the lowest and highest poles for various N. Comparing with table I, we see again that the difference with the non-periodic case is negligible for small N but increases quickly as N approaches N_{max}.

Table II.

N	y_1	y_N
1	0.005000	0.005000
2	0.004394	0.025609
3	0.004094	0.049647
4	0.003902	0.075312
5	0.003765	0.10195
10	0.003389	0.24261
20	0.003083	0.54272
50	0.002775	1.6051
100	0.002663	9.3282

4. Continuous approximation and pole condensations. We begin with the non-periodic case. The very regular distribution of poles shown in figure 4 suggests going over to a continuous approximation, with the individual poles at locations $\pm iy_j$ replaced by a density of poles $\rho(y) \geqslant 0$ normalized to the total number of poles

$$\int_{-\infty}^{+\infty} \rho(y)\, dy = 2N . \qquad (4.1)$$

Equation (3.6) is then replaced by an integral equation (the P in front of the integral means Cauchy Principal value)

$$2\nu P \int_{-\infty}^{+\infty} \frac{\rho(y')}{y - y'}\, dy' - \operatorname{sign} y = 0 . \qquad (4.2)$$

The general solution of this linear integral equation, which may be obtained by Fourier transformation, is

$$\rho(y) = \frac{1}{\pi^2 \nu} \ln \frac{c}{|y|}, \qquad (4.3)$$

where c is an arbitrary positive constant. This solution is neither normalized nor positive (for $|y| > c$).

This is not surprising : we have assumed that (4.2) is true for all y, but if the density drops to zero at a finite distance y_{max} then there is no need for (4.2) to be true for $y > y_{max}$. In fact (4.2) cannot be true for all y : for any finite distribution, the first term in (4.2) tends to zero for $y \to \infty$. Equation (4.3) only represents an inner expansion near the origin and c must be determined by matching.

One method for determining the constant c is to truncate the density (4.3) to zero beyond $|y| = c$, and to use the normalization condition (4.1). This gives

$$c = \pi^2 \nu N . \qquad (4.4)$$

From (4.3) we compute the cumulative distribution :

$$R(y) = \int_0^y \rho(u)\, du = \frac{y}{\pi^2 \nu}\left(1 + \ln \frac{c}{y}\right). \qquad (4.5)$$

The curve $R(y)$ is shown on figures 4a and 4b as a dotted line, for c given by (4.4). It reproduces correctly the shape of the observed distribution, but stays somewhat below. The optimal matching is obtained with

$$c = 1.28\, \pi^2 \nu N , \qquad (4.6)$$

which produces the dashed curve on figures 4a and 4b. There is now very good agreement, except in the outermost parts of the distribution for $N = 100$.

The discrete positions of the poles can be estimated by solving the implicit equation

$$R(y_j) = j - \tfrac{1}{2} . \qquad (4.7)$$

(This formula would give the exact pole positions if the curve $R(y)$ passed through the middle point of each vertical step in Fig. 4.) The solution for the innermost pole ($j = 1$), using (4.6) and (4.7) is given in table I, column 4. Agreement with the true value of y_1 is seen to improve slowly as N increases.

For $N \to \infty$, (4.7) gives $y_1 \to 0$, and more generally $y_j \to 0$: the concentration of poles near the origin increases without limit (*pole condensation*). It increases extremely slowly, however : y_j varies to leading order in N as $1/\ln N$. The innermost poles get squeezed in logarithmically with N due to the repulsion from all other poles.

Now we turn to the periodic case and reinsert ν. By (3.10), the maximum number of pole pairs that can be put in an equilibrium configuration is inversely proportional to ν. We observe that when entire initial data are prescribed for the Sivashinsky equation, poles are created at $t = 0_+$ at infinity in arbitrary large numbers by essentially the same mechanism that operates for the Burgers equation [10-11]. We shall therefore assume that the number of poles present in the steady state is equal to its maximum acceptable value, N_{max}. When ν is small we then get order $1/\nu$ very closely packed poles (*pole condensation*). The distribution within the condensation can again be obtained by going to the continuum limit; the

analog of equation (4.2) is

$$vP\int_{-\infty}^{+\infty}\rho(y')\coth\frac{y-y'}{2}\,dy' - \operatorname{sign} y = 0 \qquad (4.8)$$

The general solution is

$$\rho(y) = \frac{1}{\pi^2 v}\ln\left(c_1 \coth\frac{|y|}{4}\right) \qquad (4.9)$$

where c_1 is an arbitrary positive constant. This is again an inner expansion. Since we know that there is only a finite number of poles $O(v^{-1})$, we impose that the density $\rho \to 0$ as $y \to \infty$. This gives

$$c_1 = 1\,. \qquad (4.10)$$

Moreover ρ is then positive for all y and

$$\int_{-\infty}^{+\infty}\rho(y)\,dy = \frac{1}{v}\,. \qquad (4.11)$$

Since we assume N to be large and equal to the maximum value N_{max} allowed by (3.10), we have

$$\frac{1}{v} \sim 2N - 1 \sim 2N\,, \qquad (4.12)$$

so that the normalization condition (4.1) is fulfilled to leading order.

We define again the cumulative distribution as

$$R(y) = \int_0^y \rho(u)\,du\,. \qquad (4.13)$$

For ρ given by (4.9), this integral does not appear to have a closed form, so we compute it numerically. The integrand being singular at $y = 0$, it is convenient to do first an integration by parts :

$$R(y) = \frac{y}{\pi^2 v}\ln\coth\frac{|y|}{4} + \frac{1}{2\pi^2 v}\int_0^y \frac{u\,du}{\sinh u/2}\,. \qquad (4.14)$$

The singularity is then isolated in the first term, and the second term is easily evaluated numerically. The curve $R(y)$ is shown on figure 5 as a dashed line. The agreement with the observed distribution is excellent over the whole y range.

Note that for small y, the density is to leading order given by

$$\rho(y) \sim \frac{1}{\pi^2 v}\ln\frac{4}{|y|}\,. \qquad (4.15)$$

We recover the form (4.3) of the non-periodic case, with $c = 4$. The best-fit solution (4.6) for the non-periodic case, together with (4.12) would have given

$$c \simeq 0.64\,\pi^2 \simeq 6.32\,. \qquad (4.16)$$

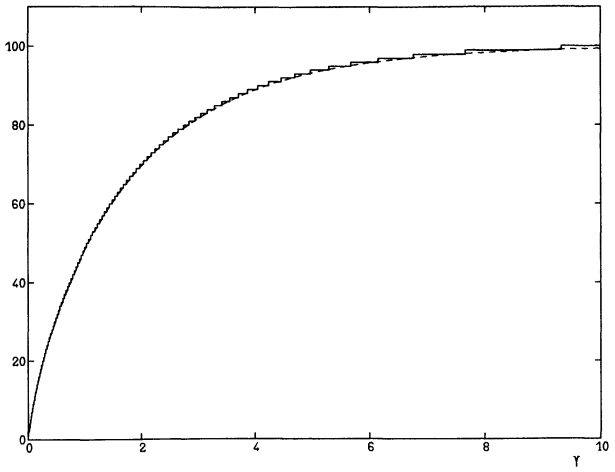

Fig. 5. — Cumulative distribution of poles along the imaginary axis in the periodic case. Full curve : discrete distribution for $v = 0.005$, $N = 100$, Dashed curve : asymptotic distribution (4.14).

Thus, for given large N, the periodic and non-periodic cases have the same functional form for $R(y)$ near $y = 0$ but different normalizations. We can again estimate the position of the innermost pole y_1 from (4.7) and (4.14); since y is small, the latter can be replaced by

$$R(y) = \frac{y}{\pi^2 v}\left(1 + \ln\frac{4}{y}\right). \qquad (4.17)$$

for $v = 0.005$, we obtain from this continuous approximation

$$y_1^* = 0.003012\,, \qquad (4.18)$$

to be compared with the value computed from the discrete case

$$y_1 = 0.002663\,. \qquad (4.19)$$

If v is varied, with N simultaneously changed so that is always has its maximum value, then y_1, the distance of the innermost pole to the real axis, is given to leading order in v by

$$y_1 \sim \frac{\pi^2 v}{2\ln(1/v)}\,. \qquad (4.20)$$

Using the above asymptotic expansions we can determine some key features of the small v steady solutions in the periodic case. The solution of the Sivashinsky equation with a pole condensation on the imaginary axis is given in real physical space by

$$u(x) = -v\sum_{\substack{n=-N\\ n\neq 0}}^{N}\cot\frac{x - iy_n}{2}\,. \qquad (4.21)$$

For $|x| \gg v/\ln(1/v)$ we can use the continuous density

and obtain

$$u(x) \sim -\frac{1}{\pi^2}\int_{-\infty}^{+\infty} \cot\frac{x-iy}{2} \ln\left[\coth\frac{|y|}{4}\right] dy. \tag{4.22}$$

The asymptotic expansion of this integral for (not too) small x gives

$$u(x) \sim \frac{1}{2\pi}\,\mathrm{sign}\,(x) \ln|x|. \tag{4.23}$$

The corresponding expansion for the flame front displacement $\phi(x)$ is

$$\phi(x) - \phi(0) \sim \frac{1}{2\pi}|x| \ln|x|. \tag{4.24}$$

Sivashinsky (1983) refers to a similar logarithmic singularity at the cusps of the flame folds, obtained by McConnaughey (1982). Actually there is no real singularity : from equation (4.20) the closest complex singularity is within a distance $y_1 = O(\nu/\ln \nu^{-1})$; thus the cusp is slightly rounded over a distance y_1.

We now calculate the spectrum $E(k)$ of the solution, defined as the squared modulus of the Fourier transform of the steady flame front displacement. Since $u(x) = \partial_x \phi(x)$ we have

$$E(k) = k^{-2} |\hat{u}_k|^2, \tag{4.25}$$

where

$$\hat{u}_k = \frac{1}{2\pi}\int_0^{2\pi} e^{-ikx} u(x)\, dx. \tag{4.26}$$

A simple residue calculation based on the pole decomposition gives, for $k > 0$

$$\hat{u}_k = 2i\nu \sum_{n=1}^{N} \exp(-ky_n). \tag{4.27}$$

For large k we must distinguish two ranges :

(i) *Dissipation range.* When $|k| y_1 \gg 1$ only the nearest pole singularity matters and we get

$$E(k) \sim 4\nu^2 k^2 \exp(-2y_1 k), \tag{4.28}$$

with y_1 given by equation (4.20).

(ii) *Inertial range.* When $1 \ll |k| \ll y_1^{-1}$ we may replace the sum in equation (4.27) by an integral over the continuous distribution of poles; this gives to leading order (for $\nu \to 0$ first and then $k \to \infty$)

$$E(k) \sim \frac{4}{\pi^4}\ln^2|k|. \tag{4.29}$$

Note that the energy spectrum for $u(x)$ follows a $k^{-2}\ln^2|k|$ law; i.e. it is somewhat shallower than the k^{-2} spectrum obtained for Burgers' model. The numerical simulation of Pumir [4] (his Fig. 5b) gives for $u(x)$ an energy spectrum that approximately follows a $k^{-\alpha}$ law with $\alpha \simeq 1.23$ which is also shallower than k^{-2}. Given that Pumir's equation is not exactly the Sivashinsky equation and given also the limited range of wavenumbers involved there is probably no genuine discrepancy.

5. Discussion.

We have found that the pole decomposition provides a reduction of the Sivashinsky equation to a discrete Dynamical System. The latter admits steady state solutions with all the poles aligned parallel to the imaginary axis. In the spatially periodic case the maximum number N of complex conjugate pairs of poles in an alignment is such that $\nu(2N-1) < 1$. We conjecture more general results for analytic periodic initial data : (i) as $t \to \infty$ all the singularities (poles and others) are pushed off to infinity, except a finite number N of pairs of poles satisfying the above inequality; (ii) for real times poles stay uniformly bounded away from the real axis. The former result has been recently established for the case of initial conditions with a finite but arbitrary number of poles [13, 14]. In this context we also mention a result of Foias, Nicolaenko, Sell and Temam [17] concerning the family of equations

$$\partial_t u + u\,\partial_x u = M_\varepsilon u, \tag{5.1}$$

where the operator M_ε has the following representation in Fourier space

$$M_\varepsilon : \hat{u}_k \mapsto [\varepsilon(|k| - k^2) + (1-\varepsilon)(k^2 - k^4)]\,\hat{u}_k. \tag{5.2}$$

It is assumed that $0 \leqslant \varepsilon \leqslant 1$; $\varepsilon = 1$ is the Sivashinsky equation. For the case of space-periodic odd solutions of equation (5.2) Foias *et al.* [15] have shown that when $t \to \infty$ the solutions have a finite dimensional attractor imbedded in a finite dimensional manifold.

In the periodic case with small ν we found that the poles on a vertical alignment condense into a ln coth distribution the signature of which in real physical space is a cusp in the flame front. This suggests a real singularity. Actually, as we have seen in section 4 there are only complex poles, but the ones nearest to the real axis are at a distance $O(\nu/\ln \nu^{-1})$ so that the cusp is slightly rounded. It is noteworthy that this distance is smaller by a factor $1/\ln \nu^{-1}$ to what would have been inferred from a naive analysis based on the observation that wavenumbers in excess of ν^{-1} are linearly stable. This discrepancy is important when attempting to numerically solve the Sivashinsky equation : the number of Fourier modes that are necessary scales like $\nu^{-1}\ln\nu^{-1}$ and not like ν^{-1}. Otherwise the numerics will work well as long as the poles stay within $O(\nu)$ of the real axis (as in the two-pole solution); after some time however the poles will start piling up vertically and spurious singularities may be observed [4].

We finally mention an open problem. We have shown that the Sivashinsky equation has stable steady solutions, which can be made trivially time-dependent by a Galilean transformation. There may also be non-trivial time-dependent solutions. In one spectral simulation with 25 linearly unstable modes ($\nu = 1/25$) we have observed a complicated time-dependent régime going through a succession of single and multi-wrinkle configurations. At the moment we cannot rule out ever-lasting, possibly chaotic, time-dependent solutions [16].

Acknowledgments.

We have benefitted from discussions with Y. C. Lee, A. Pumir, B. Nicolaenko, and S. Zaleski. Some of the numerical results reported in section 3 were obtained independently by J. P. Rivet.

Appendix A.

THE POLE DECOMPOSITION. — We wish to show that equations (1.1)-(1.3) have pole solutions of the form

$$u(t, x) = -2\nu \sum_{\alpha=1}^{2N} \frac{1}{x - z_\alpha(t)}. \qquad (A.1)$$

with

$$\dot{z}_\alpha = -2\nu \sum_{\beta \neq \alpha} \frac{1}{z_\alpha - z_\beta} - i \operatorname{sign}(\Im(z_\alpha)). \qquad (A.2)$$

We note that $u(x)$ is a linear combination of terms of the form

$$p_z(x) = \frac{1}{x - z}. \qquad (A.3)$$

We claim that

$$\Lambda p_z(x) = i \operatorname{sign}(\Im(z))\, \partial_x p_z(x), \qquad (A.4)$$

where Λ is the pseudo-differential operator defined by (1.3), i.e. multiplication by $|k|$ in Fourier space. A simple residue calculation gives the following expression for the Fourier transform $\hat{p}_z(k)$ of $p_z(x)$:

$$\text{for } \Im(z) > 0, \quad \hat{p}_z(k) = iH(-k)\, e^{-ikz}; \qquad (A.5)$$

$$\text{for } \Im(z) < 0, \quad \hat{p}_z(k) = iH(+k)\, e^{-ikz}, \qquad (A.6)$$

where $H(.)$ is the Heavyside function. Thus $\hat{p}_z(k)$ has its support in the negative or positive k-axis, depending on the sign of the imaginary part of z. Since the Fourier transform of ∂_x is the multiplication by ik (see (1.2)), the operator Λ acting on the function p_z is equivalent to $\pm i\partial_x$. This proves (A.4). We may thus interpret the operator Λ in the Sivashinsky equation (1.1) as producing an advection in the complex plane, in the imaginary direction towards the real axis.

Finally, the proof that (A.1) and (A.2) satisfies the Sivashinsky equation (1.1) is obtained by substitution and straightforward algebra, using the identity

$$\sum_{\alpha,\beta} \frac{1}{x - z_\alpha} \frac{1}{x - z_\beta} = \sum_\alpha \frac{1}{(x - z_\alpha)^2} + \sum_{\alpha \neq \beta} \frac{2}{z_\alpha - z_\beta} \frac{1}{x - z_\alpha}. \qquad (A.7)$$

Appendix B.

We give here the proofs of the assertions made in section 3. We remark first that the differential equations (3.3) may be written in terms of a Lyapunov function U:

$$\dot{y}_j = f_j = \frac{\partial U}{\partial y_j}, \qquad (B.1)$$

with, in the non-periodic case :

$$U = \nu \left[\sum_j \ln y_j + 2 \sum_{\substack{j,k \\ j<k}} (\ln(y_k - y_j) + \ln(y_k + y_j)) \right] - \sum_j y_j, \qquad (B.2)$$

and in the periodic case :

$$U = \nu \left[\sum_j \ln \sinh y_j + 2 \sum_{\substack{j,k \\ j<k}} \left(\ln \sinh \frac{y_k - y_j}{2} + \ln \sinh \frac{y_k + y_j}{2} \right) \right] - \sum_j y_j. \qquad (B.3)$$

A simple computation shows that the function $U(y_1, ..., y_N)$ has a negative curvature in every direction. Specifically, if we consider a linear displacement : $y_j = a_j + b_j v$, with a_j, b_j constants and v variable, then $d^2U/dv^2 < 0$. An immediate consequence is that there cannot exist more than one steady state : if two existed, on the straight-line segment joining them we would have $dU/dv = 0$ at each end, which is in contradiction with the above property. Another consequence is that if a steady state does exist, then it is a global maximum for U.

Next we show that a steady state actually exists (provided, in the periodic case, that the inequality (3.10) holds). We consider a sub-problem in which $y_{p+1}, ..., y_N$ have given values while $y_1, ..., y_p$ are free, and we look for a steady state for the free variables. Specifically, we look for values of $y_1, ..., y_p$ such that (3.6) is satisfied for $j = 1, ..., p$. The accessible phase

space is :

$$0 < y_1 < \cdots < y_p < y_{p+1} . \qquad (B.4)$$

The same reasoning as above shows that there cannot exist more than one equilibrium for $y_1, ..., y_p$. We show now by recursion that one exists. Consider first the case $p = 1$. The domain of variation of y_1 is $0 < y_1 < y_2$. For $y_1 \to 0$, $f_1 \to + \infty$; and for $y_1 \to y_2$, $f_1 \to - \infty$. Therefore there exists a y_1 for which f_1 vanishes, i.e., a steady state for y_1. Suppose now that we have proved the existence of a steady state for $p-1$ poles and we want to prove it for p poles, with $p < N$. We let y_p vary in the interval $0 < y_p < y_{p+1}$, with the other poles $y_1, ..., y_{p-1}$ continually adjusted to their equilibrium position. For $y_p \to 0$, $f_p \to + \infty$; and for $y_p \to y_{p+1}$, $f_p \to - \infty$ (it is easily seen that the distance $y_p - y_{p-1}$ remains finite in the limit). Therefore there exists a y_p for which $f_p = 0$.

The last case $p = N$, is treated in the same fashion but with a slight difference. The interval of variation is now $0 < y_N < \infty$. For $y_N \to \infty$, $f_N \to - 1$ in the non-periodic case, and $f_N \to \nu(2N - 1) - 1$ in the periodic case. Therefore there exists a y_N for which $y_N = 0$. This completes the proof of existence of a steady state.

Finally, we have from (B.1) :

$$\dot{U} = \sum_j \frac{\partial U}{\partial y_j} \dot{y}_j = \sum_j f_j^2 \geqslant 0 , \qquad (B.5)$$

the equality being obtained only at a steady state. Thus U always increases with time, except at equilibrium. On the other hand, U is bounded from above by its value at the steady state, which is a global maximum. Therefore U is a genuine Lyapunov function, and every solution of (3.3) tends toward the steady state for $t \to \infty$. This completes the proof of stability for pole-displacements parallel to the imaginary axis. This result has been extended to arbitrary displacements other than the trivial ones where all the poles undergo a same real translation [17].

References

[1] SIVASHINSKY, G. I., *Acta Astronaut.* **4** (1977) 1177.

[2] SIVASHINSKY, G. I., *Ann. Rev. Fluid Mech.* **15** (1983) 179.

[3] MICHELSON, D. M. and SIVASHINSKY, G. I., *Acta Astronaut.* **4** (1977) 1207.

[4] PUMIR, A., *Phys. Rev.* **A 31** (1985) 543.

[5] LEE, Y. C. and CHEN, H. H., *Phys. Scr.* **T 2** (1982) 41.

[6] BENJAMIN, T. B., *J. Fluid Mech.* **25** (1966) 241.

[7] ONO, H., *J. Phys. Soc. Japan* **39** (1975) 1082.

[8] FRISCH, U. and MORF, R., *Phys. Rev.* **A 23** (1981) 2673.

[9] SHRAIMAN, B. and BENSIMON, D., *Phys. Rev.* **A 30** (1984) 2840.

[10] BESSIS, D. and FOURNIER, J. D., *J. Physique Lett.* **45** (1984) L-833.

[11] FRISCH, U. in Proceed. *Sixth Kyoto Summer Institute on Chaos and Statistical Methods*, ed. Y. Kuramoto, p. 211, Springer series in Synergetics, Springer (1984).

[12] MCCONNAUGHEY, H. V., *Combust. Sci. Technol.* **33** (1983) 113.

[13] LEE, Y. C., CHENG, H. H., LEE, T. T. and QIAN, S. N., *Solitons and Turbulence ; Chaos in Infinite Dimensional Systems* ; Proc. Second Intern. Workshop on Non Linear and Turbulent Processes in Physics ; Kiev, October 1983, p. 1425, Gordon and Breach.

[14] LEE, Y. C., private communication (1985).

[15] FOIAS, C., NICOLAENKO, B., SELL, G. and TEMAM, R., *Inertial Manifold for the Kuramoto-Sivashinsky equation*, preprint Indiana University, Depart. Math. (1984).

[16] MICHELSON, D. M. and SIVASHINSKY, G. I., *Combust. Flame* **48** (1982) 211.

[17] RIVET, J. P., private communication (1985).